JACS
JOURNAL OF THE AMERICAN CHEMICAL SOCIETY
Article
pubs.acs.org/JACS

Rational Design of a Fluorescent Sensor to Simultaneously Determine Both the Enantiomeric Composition and the Concentration of Chiral Functional Amines

Kaili Wen,[†] Shanshan Yu,*[,†] Zeng Huang,[†] Liming Chen,[†] Meng Xiao,[†] Xiaoqi Yu,*[,†] and Lin Pu*[,†,‡]

[†]Key Laboratory of Green Chemistry and Technology, Ministry of Education, College of Chemistry, Sichuan University, Chengdu, China 610064

[‡]Department of Chemistry, University of Virginia, Charlottesville, Virginia 22904-4319, United States

Supporting Information

ABSTRACT: A fluorescent molecular probe, a 1,1′-bi-2-naphthol (BINOL)-based bis(naphthylimine) compound (*R*)-**4**, is designed to exhibit very different fluorescent responses at two emission wavelengths toward a variety of chiral functional amines including diamines, amino alcohols, and amino acids. At one emission wavelength (λ_1), it shows high sensitivity toward the substrates, and at another wavelength (λ_2), it shows high enantioselectivity. This is the first rational design of such a dual responsive fluorescent sensor which can be used to simultaneously determine both the concentration and the enantiomeric composition of functional chiral amines by one fluorescent measurement. This strategy is potentially generally applicable for the construction of sensors for rapid assay of structurally diverse chiral substrates. When (*R*)-**4** is treated with various chiral functional amines in the presence of $Zn(OAc)_2$, its 2-naphthylamine units are displaced off to show large fluorescent enhancement at λ_1 = 427 nm (I_1) due to the restored emission of 2-naphthylamine. The combination of the remaining chiral binaphthyl unit with the chiral substrates leads to highly enantioselective fluorescent enhancement at λ_2 > 500 nm (I_2). Since I_1 is only concentration dependent but independent of the chiral configuration, it allows the determination of the substrate concentration. The highly enantioselective I_2 allows the determination of the enantiomeric composition. Thus, using one fluorescent probe with one fluorescent measurement, both the concentration and the enantiomeric composition are determined. The dual responsive mechanism of (*R*)-**4** is studied by using various spectroscopic methods including fluorescence, UV−vis, NMR, and mass analyses.

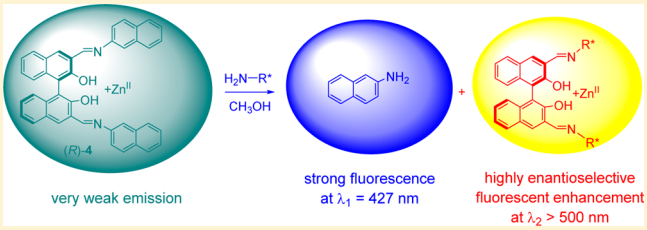

INTRODUCTION

Enantioselective fluorescent sensors are potentially useful for the rapid analysis of the enantiomeric composition of chiral compounds. In recent years, significant research has been conducted in this area, and a number of highly enantioselective fluorescent sensors have been obtained for the recognition of chiral α-hydroxycarboxylic acids, amino alcohols, and amino acids.[1,2] Because both the concentration of a substrate and its enantiomeric composition can greatly affect the fluorescent response of an enantioselective fluorescent sensor, two independent methods are generally required in order to determine these parameters.[3] In order to apply an enantioselective fluorescent sensor to high-throughput chiral assay, it is highly desirable to simultaneously determine both the concentration and the enantiomeric composition of a chiral substrate with one fluorescent measurement.[4]

Recently, our laboratory reported the use of the 1,1′-bi-2-naphthol (BINOL)-based trifluoromethyl ketone (*S*)-**1** in the fluorescent recognition of chiral diamines.[4b] It was found that the nonfluorescent (*S*)-**1** exhibits dual fluorescent enhancement at λ_1 = 370 nm and λ_2 = 438 nm upon interaction with the two enantiomers of *trans*-1,2-cyclohexanediamine. At λ_1, (*S*)-**1** shows large fluorescent enhancement toward both enantiomers with little enantioselectivity, and at λ_2, it shows high enantioselectivty with (*R*,*R*)-*trans*-1,2-cyclohexanediamine enhancing the fluorescence much greater than the (*S*,*S*)-enantiomer. Thus, the fluorescent response at λ_1 allows the determination of the total concentration of the chiral diamine and that at λ_2 allows the determination of the enantiomeric composition. Currently, this is the only report that one fluorescent sensor can be used to simultaneously determine both concentration and enantiomeric composition.

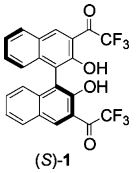

(*S*)-**1**

Although (*S*)-**1** is found to be useful for the enantioselective recognition of only certain chiral diamines and its dual

Received: January 30, 2015
Published: March 19, 2015

ACS Publications © 2015 American Chemical Society

DOI: 10.1021/jacs.5b01049
J. Am. Chem. Soc. 2015, 137, 4517−4524

responsive mechanism is also not generally applicable for the detection of other chiral molecules, this discovery has prompted us to propose a potentially general strategy to convert an enantioselective fluorescent sensor to a dual responsive fluorescent sensor that could simultaneously determine both the concentration and the enantiomeric composition of chiral compounds. As shown in Scheme 1, an

Scheme 1. A Proposed General Strategy To Convert an Enantioselective Fluorescent Sensor to a Dual Responsive Sensor

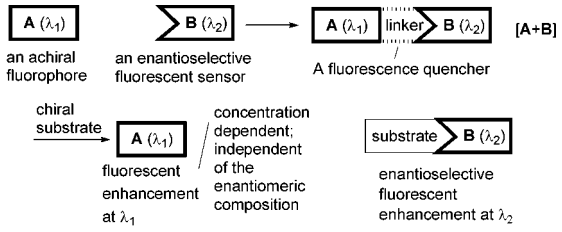

achiral fluorophore **A** with emission at λ_1 will be connected with an enantioselective fluorescent sensor **B**. The criterion for **B** to be selected is that this sensor shows enantioselective fluorescent enhancement upon interaction with a chiral substrate at a distinctively different wavelength λ_2. An appropriate linkage between **A** and **B** will be introduced so that the fluorescence of **A** is quenched in the [**A** + **B**] diad. A linkage cleavage mechanism will also be incorporated to allow the addition of a chiral substrate to release **A** and restore its emission at λ_1. Thus, the fluorescent enhancement at λ_1 should be strongly correlated with the concentration of the substrate but much less effected by its enantiomeric composition. After cleavage of the linkage, the resulting **B** should exhibit enantioselective fluorescent enhancement at λ_2 upon binding with the enantiomers of the substrate. Therefore, the [**A** + **B**] diad could allow determination of the substrate concentration at λ_1 and the enantiomeric composition at λ_2. That is, one fluorescent measurement should give both parameters.

In this paper, we wish to report a successful demonstration of the above strategy in the development of a dual responsive fluorescent sensor. We found that using such a sensor, both the concentration and the enantiomeric composition of a variety of chiral functional amines including amino alcohols, diamines, and amino acids can be simultaneously determined.

RESULT AND DISCUSSION

Design and Synthesis of a Dual Responsive Sensor (*R*)-4. We recently reported that the BINOL-based dialdehyde (*R*)-**2** in combination with Zn^{2+} is a generally useful enantioselective fluorescent sensor for chiral functional amines such as diamines, amino alcohols, and amino acids.[5] When treated with chiral functional amines in the presence of Zn^{2+}, (*R*)-**2** shows highly enantioselective fluorescent enhancement at λ > 500 nm (λ_2). In order to convert this compound to a dual responsive fluorescent sensor according to the proposed strategy in Scheme 1 for the simultaneous concentration and enantiomeric composition determination, we conducted the condensation of (*R*)-**2** with 2-naphthylamine (**3**) to generate the corresponding Schiff base (*R*)-**4** (Scheme 2). It was found that the strong emission of **3** at 427 nm (λ_1) is greatly quenched in (*R*)-**4** probably due to the intramolecular hydrogen bonding in this compound between the BINOL

Scheme 2. Preparation of Compound (*R*)-4

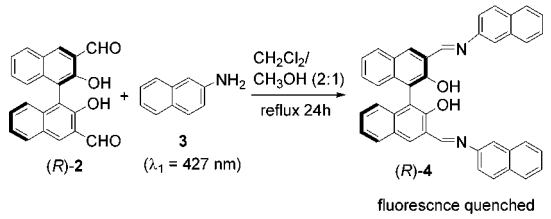

hydroxyl groups and the imine nitrogens. This indicates that compound (*R*)-**4** might be useful as the proposed diad [**A** + **B**] sensor shown in Scheme 1. We envision that upon treatment with chiral functional amines in the presence of Zn^{2+}, the 2-naphthylamine unit of (*R*)-**4** could be displaced by the more basic aliphatic amines to restore the emission at 427 nm (λ_1), and the resulting new imine-Zn^{II} complexes formed with the chiral amines should show enantioselective fluorescent response at λ > 500 nm (λ_2) as we reported for the direct use of (*R*)-**2** + Zn^{II} in chiral amine sensing.

Study of the Fluorescent Response of (*R*)-4 toward *trans*-1,2-Cyclohexanediamine in the Presence of Zn(II). We tested the above proposal by first studying the fluorescent response of (*R*)-**4** toward the enantiomers of *trans*-1,2-cyclohexanediamine, (*S*,*S*)- and (*R*,*R*)-**5**, in the presence of Zn^{2+}. When (*R*)-**4** (2.0×10^{-5} M in CH_3OH/2% CH_2Cl_2) was treated with $Zn(OAc)_2$ (4.0×10^{-5} M), it gave a weak emission signal at 555 nm attributed to the interaction of Zn^{2+} with the imine units (Figure 1). When the (*R*)-**4** + Zn^{II} solution was

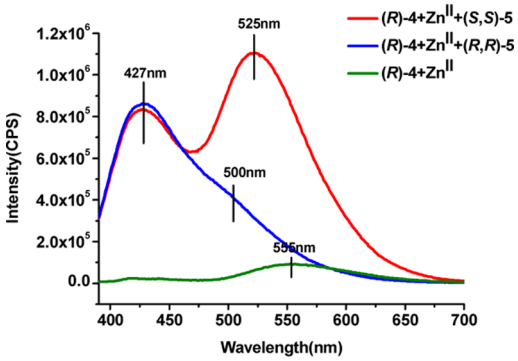

Figure 1. Fluorescence spectra of (*R*)-**4** (2.0×10^{-5} M in CH_3OH/2% CH_2Cl_2) with $Zn(OAc)_2$ (2 equiv) (green) in the presence of (*S*,*S*)-**5** (7.5 equiv) (red) or (*R*,*R*)-**5** (7.5 equiv) (blue). (λ_{exc} = 370 nm, slit = 5 nm/5 nm).

treated with (*S*,*S*)-**5** (1.5×10^{-4} M), a large fluorescence enhancement was observed with dual emissions at λ_1 = 427 nm and λ_2 = 525 nm. When the enantiomer (*R*,*R*)-**5** was used to interact with (*R*)-**4**, the same large fluorescent enhancement at λ_1 = 427 nm was observed, but the fluorescent enhancement at λ_2 was much smaller. Thus, a dual responsive fluorescent sensor is obtained for the recognition of the chiral amine. As shown in Figure 1, the emission at λ_1 is independent of the chiral configuration, and the emission at λ_2 is highly enantioselective.

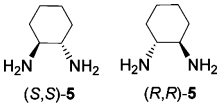

DOI: 10.1021/jacs.5b01049
J. Am. Chem. Soc. 2015, 137, 4517−4524

Scheme 3 shows a proposed explanation for the observed dual responsive fluorescent recognition. The imine metathesis

Scheme 3. A Proposed Imine Metathesis for the Reaction of (*R*)-4 + Zn^{II} with a Chiral Amine

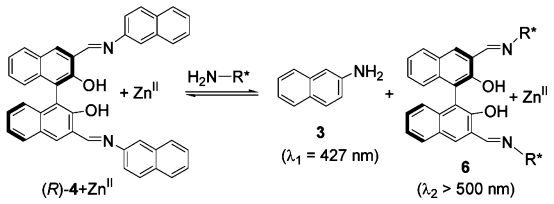

of the (*R*)-**4** + Zn^{II} complex with the chiral amine should release 2-naphthylamine to restore its emission at λ_1 = 427 nm. We found that the presence of Zn^{2+} does not change the fluorescence of 2-naphthylamine (see Figure S2). The new BINOL-imine-Zn^{II} complex **6** formed from the reaction with the chiral amine gives the enantioselective emission at λ > 500 nm matching those we reported with the direct use of the dialdehyde (*R*)-**2** in the presence of Zn^{2+}.

The effect of the concentration of the two enantiomers of the chiral diamine on the fluorescent response of the (*R*)-**4** + Zn^{II} sensor solution is shown in Figure 2a,b. As the concentrations of the enantiomers of the chiral diamine **5** (5−20 equiv) increased, the fluorescent intensities at both λ_1 and λ_2 increased. Figure 2c plots the fluorescent intensity of (*R*)-**4** + Zn^{II} at λ_1 = 427 nm (I_{427}) against the concentrations of (*S*,*S*)- and (*R*,*R*)-**5**. As shown in this plot, both enantiomers of the diamine give similar fluorescent enhancement at λ_1. Thus, I_{427} is strongly correlated with the concentration of the diamine and mostly independent of its chiral configuration. Figure 2d plots the fluorescent intensity of (*R*)-**4** + Zn^{II} at λ_2 = 525 nm (I_{525}) against the concentrations of (*S*,*S*)- and (*R*,*R*)-**5**, which shows highly enantioselective fluorescent response. Figure 2e plots the fluorescence intensity ratio I_{525}/I_{500} versus the concentration of the chiral diamine. When more than 7.5 equiv of the diamine was added, the ratio I_{525}/I_{500} for (*S*,*S*)-**5** remains constant at 1.21 and that for (*R*,*R*)-**5** at 0.73. That is, when the concentration of the diamine is greater than 7.5 equiv of (*R*)-**4**, the fluorescent intensity ratio I_{525}/I_{500} is only determined by the chiral configuration but independent of the concentration.

We also prepared (*S*)-**4**, the enantiomer of (*R*)-**4**, and studied the effects of the concentration of the chiral diamine **5** on the fluorescent responses of (*S*)-**4** + Zn^{II} at λ_1 and λ_2. Similar fluorescence enhancement at λ_1 and mirror image relationship at λ_2 with Figure 2 confirmed the enantioselective fluorescent recognition (Figure S3).

We then tested the interaction of the (*R*)-**4** + Zn^{II} sensor solution with the diamine **5** at varying concentration and enantiomeric composition, and the results are shown in Figure 3. We have plotted I_{525}/I_{500} of (*R*)-**4** + Zn^{II} versus (*S*,*S*)-**5** % from 7.5 to 12.5 equiv in Figure 3a. In this plot, the curves of different concentrations of the diamine nearly overlap with one another. Therefore, the enantiomeric purity of the chiral diamine can be directly determined by measuring the fluorescence intensity ratio I_{525}/I_{500}.

Since I_{427} is strongly correlated with the concentration of both (*S*,*S*)- and (*R*,*R*)-**4**, we plotted I_{427} of (*R*)-**4** + Zn^{II} versus the total concentration of **5** at varying enantiomeric compositions in Figure 3b. In this plot, all the curves are very close to each other, indicating that the chiral configuration

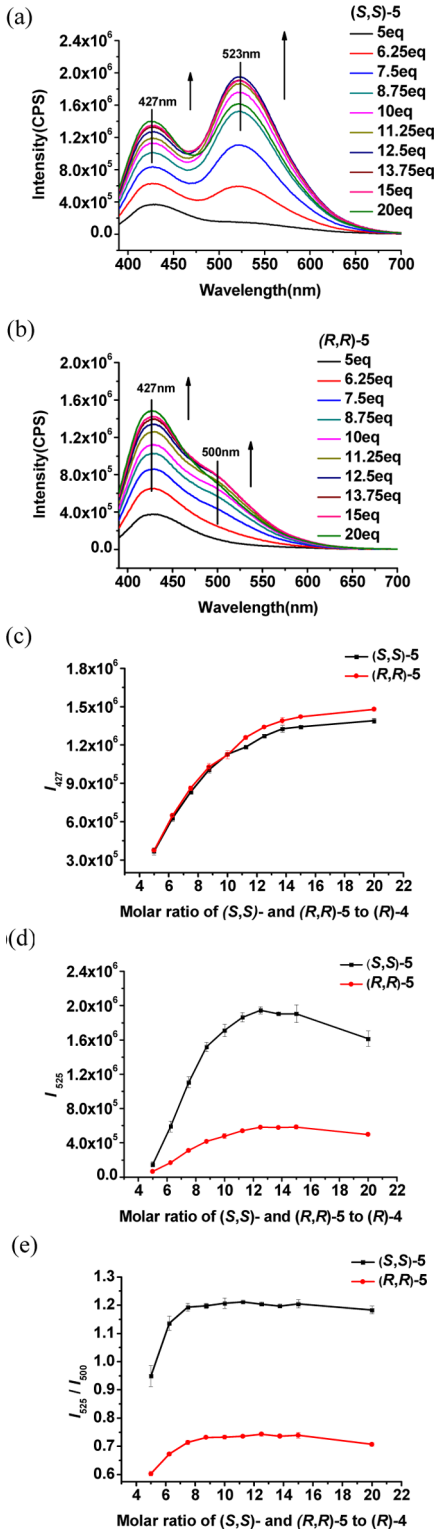

Figure 2. Fluorescent response of (*R*)-**4** (2.0×10^{-5} M in CH_3OH/2% CH_2Cl_2) + Zn^{II} (2 equiv) toward 5−20 equiv (*S*,*S*)-**5** (a) and (*R*,*R*)-**5** (b). Plots of I_{427} (c), I_{525} (d), and I_{525}/I_{500} (e) versus the concentrations of (*S*,*S*)-**5** and (*R*,*R*)-**5**. (λ_{exc} = 370 nm, slit: 5/5 nm).

of the diamine has little effect on I_{427}. Thus, I_{427} can be used to determine the total concentration of chiral diamine **5**. Therefore, both the concentration and the enantiomeric composition of the chiral diamine can be simultaneously

DOI: 10.1021/jacs.5b01049
J. Am. Chem. Soc. 2015, 137, 4517−4524

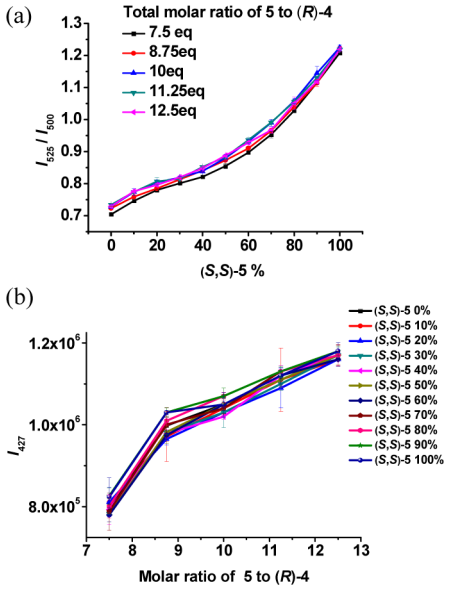

Figure 3. Fluorescent response of (*R*)-**4** (2.0×10^{-5} M in CH_3OH/2% CH_2Cl_2) + Zn^{II} (2 equiv) toward **5** at varying concentration and enantiomeric composition. (a) I_{525}/I_{500} versus (*S*,*S*)-**5** % at various concentrations. (b) I_{427} versus the concentrations of **5** at various enantiomeric compositions. (λ_{exc} = 370 nm, slit: 5/5 nm).

determined by one fluorescence measurement with the use of the (*R*)-**4** + Zn^{II} probe.

We have applied Figure 3a,b to determine both the enantiomeric composition and the concentration of five samples of the chiral diamine **5**, and the results are summarized in Table 1. As shown in the table, the correlation coefficient of

Table 1. Correlation of the Actual Enantiomeric Composition of Five Samples of 5 with Those Determined by Using the Fluorescent Sensor[a]

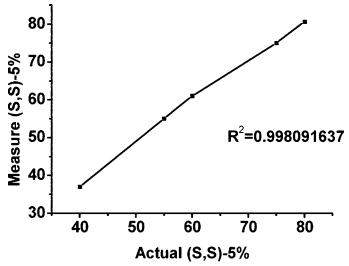

sample (*S*,*S*)-**5**%	measured by sensor	error (%)	sample conc.	measured by sensor	error (%)
40	37	7.5	16.25	16.5	1.5
80	80.6	0.8	18.75	19.37	3.3
55	55	0	20	21.25	6.3
60	61	1.7	21.25	21.75	2.4
75	75	0	22.5	23.5	5.6

[a]Data of the actual concentration and enantiomeric composition versus those determined by using Figure 3a,b.

known enantiomeric compositions versus those measured by our fluorescent method is 0.998. The values of (*S*,*S*)-**5**% and the total concentration of the diamine measured by using the fluorescent sensor had average errors of 2% and 3.8%, respectively. These data indicate that the accuracy of this fluorescent method is adequate for the desired application.

Study of the Fluorescent Response of (*R*)-4 toward Chiral Amino Alcohols in the Presence of Zn^{2+}. We studied the interaction of the (*R*)-**4** + Zn^{II} sensor with chiral amino alcohols, including phenylglycinol (**7**), phenylalaninol (**8**), and alaninol (**9**). All of these amino alcohols caused dual fluorescent responses to the sensor, similar to the diamine **5**. For example, as shown in Figure 4a,b, addition of 10−70 equiv of *L*-**7** to the mixed solution of (*R*)-**4** (2.0×10^{-5} M in CH_3OH/2% CH_2Cl_2) and Zn^{II} (2 equiv) induced fluorescent enhancement at λ_1 = 427 nm and λ_2 = 527 nm. Although *D*-**7** also enhanced emissions at 427 and 505 nm as well, the emission at 505 nm was much lower than that caused by *L*-**7**.

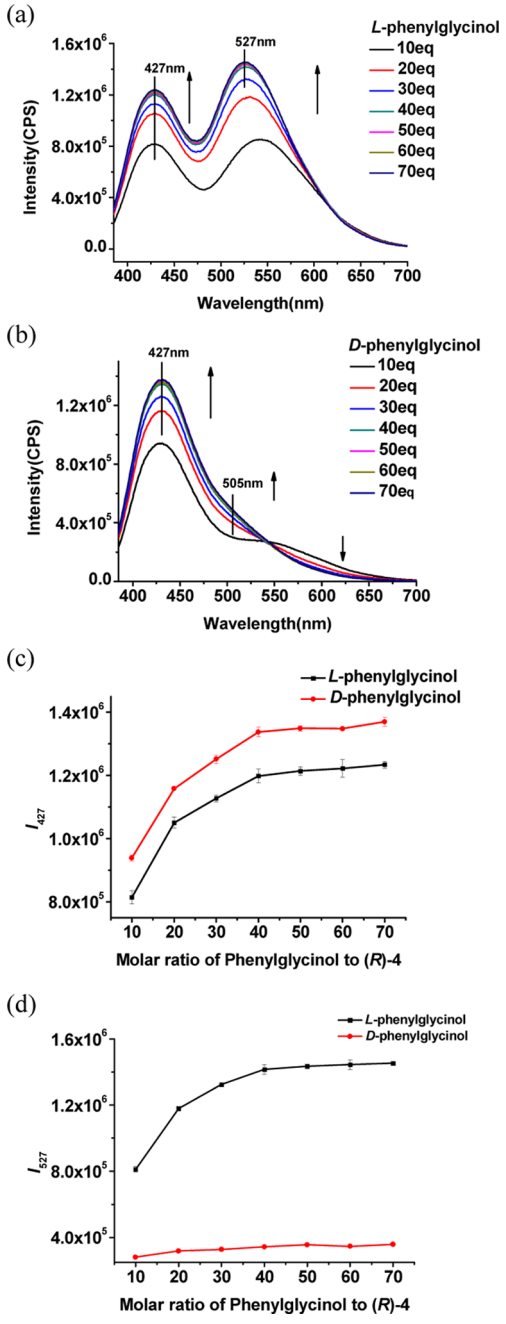

Figure 4. Fluorescent response of (*R*)-**4** (2.0×10^{-5} M in CH_3OH/2% CH_2Cl_2) + Zn^{II} (2 equiv) toward *L*-**7** (a) and *D*-**7** (b). I_{427} (c) and I_{527} (d) versus the concentrations of *L*-**7** and *D*-**7**. (λ_{exc} = 365 nm, slit: 4/4 nm).

DOI: 10.1021/jacs.5b01049
J. Am. Chem. Soc. 2015, 137, 4517−4524

Figure 4c plots the fluorescent intensity I_{427} of (*R*)-**4** + Zn^{II} at λ = 427 nm against the varying concentrations of *L*- and *D*-**7**. It shows that the chiral configuration of the amino alcohol has certain effect on I_{427}. Figure 4d plots I_{527} versus the concentration of *L*- and *D*-**7** which shows highly enantioselective response. The results for the interaction of the (*R*)-**4** + Zn^{II} sensor with chiral amino alcohols **8** and **9** are included in Figures S4−S7.

We then studied the interaction of the (*R*)-**4** (2.0×10^{-5} M in CH_3OH/2% CH_2Cl_2) + Zn^{II} (2 equiv) sensor solution with **7** at varying concentration and enantiomeric composition. In Figure 4c, it is shown that the chiral configuration of the amino alcohol has certain effect on I_{427}. In order to take this effect into consideration in the concentration determination, we have obtained the 3D plot of I_{427}, I_{527} and concentration of **7** (Figure 5a) in which I_{527} is strongly correlated with the chiral

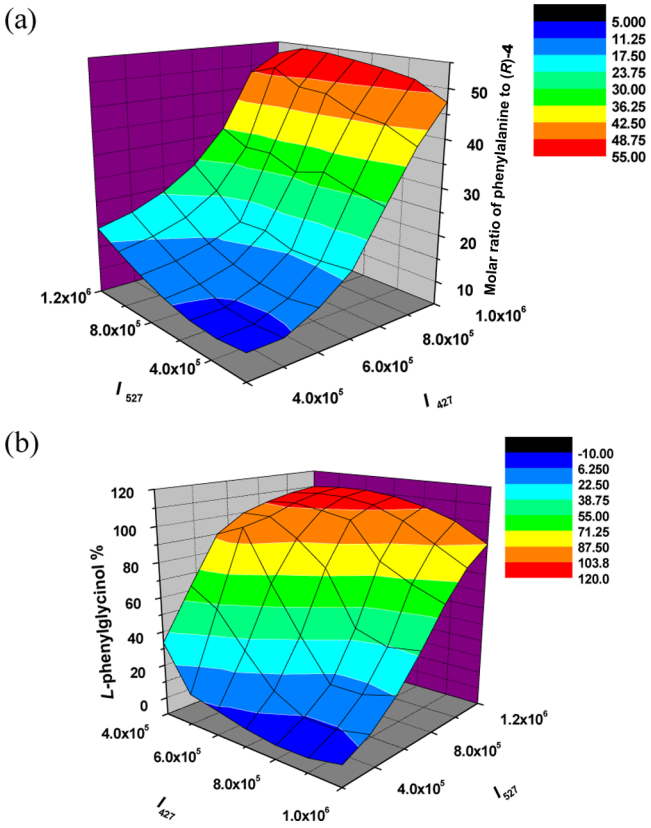

Figure 5. Fluorescent response of (*R*)-**4** (2.0×10^{-5} M in CH_3OH/2% CH_2Cl_2) + Zn^{II} (2 equiv) toward **7** of varying concentration and enantiomeric composition. (a) I_{427}, I_{527} versus the total concentration of **7**. (b) I_{427}, I_{527} versus the enantiomeric composition (*S*,*S*)-**7**%. (λ_{exc} = 365 nm, slit: 4/4 nm).

configuration of the substrate. Thus, the concentration of **7** with varying enantiomeric composition can be determined by using Figure 5a. A 3D plot of I_{427}, I_{527} and (*S*,*S*)-**7**% is also obtained in Figure 5b which can be used to determine the enantiomeric composition of **7** with varying concentration. Therefore, these 3D plots allow simultaneous determination of both concentration and enantiomeric composition with one fluorescent measurement.

Study of the Fluorescent Response of (*R*)-4 toward Chiral Amino Acids in the Presence of Zn(II). We studied the interaction of (*R*)-**4** + Zn^{II} with chiral amino acids **10** − **14** by treatment of the solution of (*R*)-**4** (2.0×10^{-5} M in CH_3OH/2% CH_2Cl_2) + Zn^{II} (2 equiv) with amino acid + *n*-Bu_4NOH solutions (amino acid/*n*-Bu_4NOH 1:1.1) in methanol. Figure 6a shows that there were large fluorescent

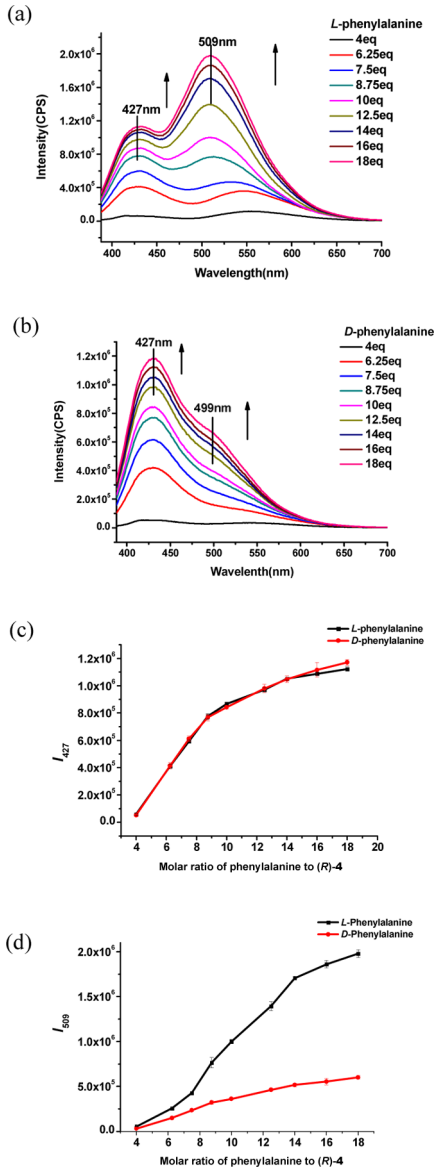

Figure 6. Fluorescent response of (*R*)-**4** (2.0×10^{-5} M in CH_3OH/2% CH_2Cl_2) + Zn^{II} (2 equiv) to *L*-**10** (a) and *D*-**10** (b). Plots of I_{427} (c) and I_{509} (d) versus the concentrations of *L*-**10** and *D*-**10**. (λ_{exc} = 368 nm, slit: 5/5 nm).

enhancements at λ_1 = 427 nm and λ_2 = 509 nm when the (*R*)-**4** + Zn^{II} solution was treated with *L*-phenylalanine (**10**) in the presence of *n*-Bu_4NOH. Under the same conditions, the enantiomer *D*-**10** gave similar fluorescent enhancement at λ_1 = 427 nm but much smaller enhancement at the long wavelength emission (Figure 6b). As shown in Figure 6c, the chiral configuration of the amino acid has little effect on I_{427}. Figure 6d plots I_{509} versus the concentration of *L*- and *D*-**10** which shows very good enantioselective response.

We measured the fluorescent response of the (*R*)-**4** (2.0×10^{-5} M in CH_3OH/2% CH_2Cl_2) + Zn^{II} (2 equiv) sensor solution toward the *n*-Bu_4NOH solution of **10** at varying concentration and enantiomeric composition. A 3D plot of I_{509},

DOI: 10.1021/jacs.5b01049
J. Am. Chem. Soc. 2015, 137, 4517−4524

I_{427} and *L*-phenylalanine% is obtained (Figure 7). This plot can be used to determine the enantiomeric composition of the amino acid of varying concentration. Since I_{427} is only dependent on the concentration of the amino acid and independent of its chiral configuration as shown in Figure 6c, it can be used directly to determine the concentration of the amino acid.

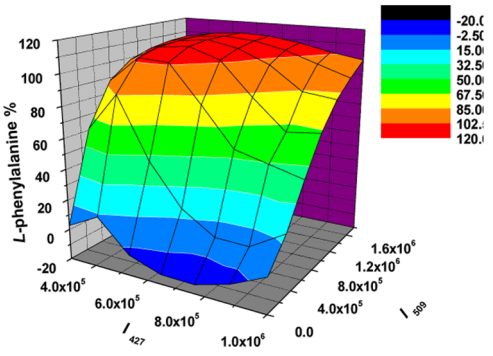

Figure 7. Fluorescent responses of I_{427} and I_{509} versus the enantiomeric composition of **10** for the interaction of (*R*)-**4** (2.0×10^{-5} M in CH_3OH/2% CH_2Cl_2) + Zn^{II} (2 equiv) with **10** of varying concentration and enantiomeric composition. (λ_{exc} = 368 nm, slit: 5/5 nm).

The interaction of the sensor solution with other amino acids such as the aliphatic amino acid alanine (**11**), the acidic amino acid glutamic acid (**12**), the basic amino acid histidine (**13**), and the γ-hydroxyl amino acid serine (**14**) were investigated. Similar to that observed for **10**, these amino acids in the presence of *n*-Bu_4NOH caused fluorescent enhancements at λ_1 = 427 nm and λ_2 > 500 nm. The enhancements at λ_1 were similar for the two enantiomers of each amino acid at the same concentration. The enhancements at λ_2 are different for different amino acids with various enantioselective responses (see Figures S8–S11). These dual responsive fluorescent enhancements can allow simultaneous determination of both concentration and enantiomeric composition.

Additional Spectroscopic Studies for the Reaction of (*R*)-4 with (*S,S*)- and (*R,R*)-5 in the Presence of Zn^{2+}. In order to gain further understanding on the use of (*R*)-**4** in the fluorescent recognition of the chiral functional amines, we conducted additional spectroscopic studies for the reaction of (*R*)-**4** with the chiral diamine **5** in the presence of Zn^{2+}.

UV–vis Study. The UV spectrum of the solution of (*R*)-**4** + Zn^{II} in methanol exhibited absorptions at λ_{max} (ε) = 223 (1.05×10^6), 255 (7×10^5), and 356 (3.7×10^5) nm (Figure 8a). Coordination of Zn(II) to (*R*)-**4** does not significantly change the UV absorption. With the increase of the concentration of (*S,S*)- and (*R,R*)-**5**, there were large absorption decreases at λ_{max} = 223 and 356 nm with increasing new absorptions at λ_{max} = 217, 240, 265, and 410 nm (Figures 8a and S12). Unlike that observed in fluorescent study, both enantiomers of the diamine generated the same UV absorption responses from the sensor. In Figure 8b, we compared the fluorescent spectra of the aldehyde (*R*)-**2** + Zn^{II} + (*R,R*)-**5**, 2-naphthylamine, (*R*)-**4** + Zn^{II} + (*R,R*)-**5**, and (*R*)-**4** + Zn^{II} under the same conditions. It shows that the spectrum of (*R*)-**4** + Zn^{II} + (*R,R*)-**5** is equivalent to the sum of those of (*R*)-**2** + Zn^{II} + (*R,R*)-**5** and 2-naphthylamine. This supports the reaction shown in Scheme 3 proposed on the basis of the fluorescent study.

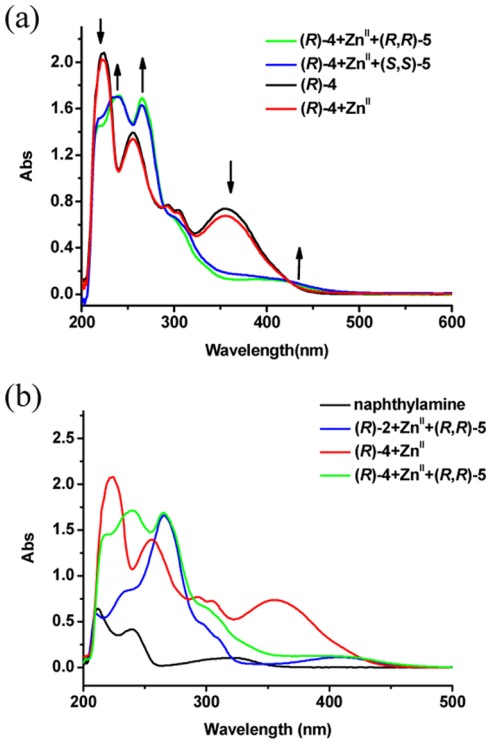

Figure 8. (a) UV–vis absorption spectra of (*R*)-**4** (2.0×10^{-5} M in CH_3OH/2% CH_2Cl_2) + Zn^{II} (2 equiv) with/without (*S,S*)- and (*R,R*)-**5** (12 equiv). (b) UV–vis absorption spectra of (*R*)-**2** and (*R*)-**4** with (*R,R*)-**5** in the presence of Zn^{II}.

Mass Spectroscopic Study. We conducted a TOF mass spectroscopic (ES+) analysis of the product mixture after the reaction of (*R*)-**4** (2.0×10^{-3} M in 3:1 CH_3OH/CH_2Cl_2) + Zn^{II} (1.5 equiv) with (*S,S*)-**5** (7 equiv) for 12 h (Figure S13). The mass spectrum shows a peak at m/z = 535 (5.6) assigned to the imine metathesis product (**15** + H)$^+$ and a peak at m/z = 630 (75) assigned to a zinc complex **16**$^+$ generated with the addition of CH_3OH to one of the imine units. The base peak at m/z = 564 (100) is assigned to compound (**17** + H)$^+$ indicating a partial imine metathesis under the conditions. Peaks at m/z = 841 (12.5) and 1341 (16.9) are assigned to the macrocycles (**18** + H)$^+$ and **19**$^+$, respectively (Figure 9). Another peak at m/z = 740 (9.7) is assigned to the zinc complex (**20** − H)$^+$ formed from the coordination of **17** with a zinc center and another molecule of (*S,S*)-**5**.

We also analyzed the product mixture formed from the reaction of (*R*)-**4** (2.0×10^{-3} M in 3:1 CH_3OH/CH_2Cl_2) + Zn^{II} (1.5 equiv) with (*R,R*)-**5** (7 equiv) by using the TOF mass spectroscopy (ES+) (Figure S14). It gave a peak at m/z = 535 (9.7) corresponding to a compound like (**15** + H)$^+$, a peak at m/z = 630 (100) similar to the zinc complex **16**$^+$, and a peak at m/z = 564 (95.5) similar to compound (**17** + H)$^+$. However, almost no macrocyclic peaks at m/z = 841 and 1341 were found in contrast to the reaction of (*S,S*)-**5**. A peak at m/z = 740 (19.8) is observed similar to compound (**20** − H)$^+$. Thus, the mass spectroscopic analysis confirms the displacement of the 2-naphthylamine unit by the chiral diamine in the reaction with (*R*)-**4** + Zn^{II}. The observed enantioselective fluorescent response of (*R*)-**4** + Zn^{II} toward the chiral diamine could be attributed to the different product distribution generated from the reaction with the two enantiomers. This is similar to that we

DOI: 10.1021/jacs.5b01049
J. Am. Chem. Soc. 2015, 137, 4517–4524

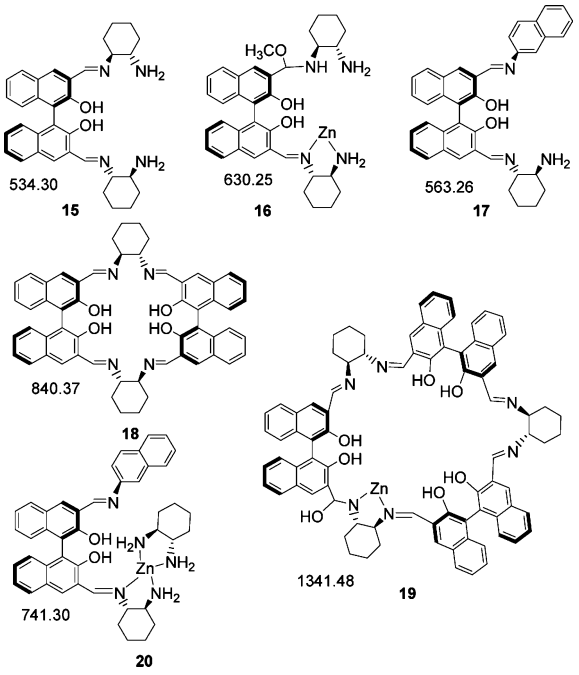

Figure 9. Proposed product structures for the reaction of (*R*)-**4** + Zn^{II} with (*S*,*S*)-**5** and their exact mass data.

observed earlier for the reaction of the aldehyde (*R*)-**2** + Zn^{II} with the enantiomers of the chiral diamine.

NMR Study. We conducted ^1H NMR analyses for the reaction of (*R*)-**4** with (*S*,*S*)- and (*R*,*R*)-**5** in the presence of Zn^{II}. To an NMR tube containing (*R*)-**4** (7.5 mM in $CDCl_3$, 0.4 mL) and 2 equiv of $ZnBr_2$ (60 mM in CD_3OD, 0.1 mL), different concentrations of (*S*,*S*)- and (*R*,*R*)-**5** in CD_3OD were added, and the total volume was made up to 0.6 mL with CD_3OD. The final concentration of (*R*)-**4** was 5 mM in $CDCl_3/CD_3OD$ (2:1). The solutions were mixed for 3 h before the ^1H NMR spectra were taken (Figures S15−17). It was found that the addition of Zn^{2+} to (*R*)-**4** did not change its ^1H NMR signals (Figure 10). This indicates that the coordination

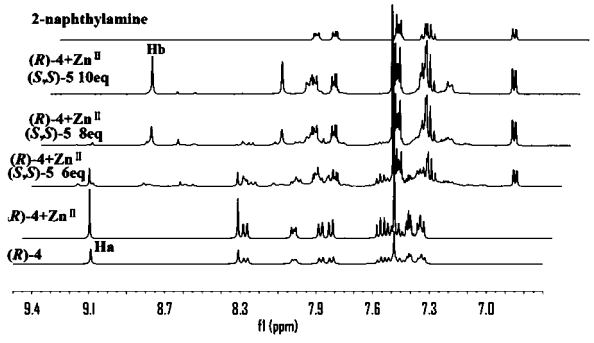

Figure 10. ^1H NMR spectra for the interaction of (*R*)-**4** with Zn^{II} and (*R*)-**4** + Zn^{II} with (*S*,*S*)-**5** in $CDCl_3/CD_3OD$ (2:1).

of (*R*)-**4** with Zn^{II} may be too weak to cause any change in the NMR signals. Reaction of (*R*)-**4** + Zn^{II} with excess amount of the diamine (*S*,*S*)-**5** converted the aromatic imine (H_a) to an aliphatic imine (H_b) with the release of 2-naphthylamine.

All the above spectroscopic studies indicate that the reaction of (*R*)-**4** with the diamine in the presence of Zn^{II} occurs with an imine metathesis process leading to the displacement of the 2-naphthylamine unit. They demonstrate that an aromatic amine unit can be easily displaced with an aliphatic amine unit, and this process can be used for the detection of the functional amines.

Summary. We have demonstrated that for the first time an enantioselective fluorescent sensor can be rationally converted to a dual responsive fluorescent sensor to simultaneously determine both the concentration and the enantiomeric composition of a chiral substrate. Such a sensor can greatly facilitate the rapid assay of chiral compounds. The design principle presented in this paper represents a potentially general strategy for the development of dual responsive fluorescent sensors. As shown in this work, compound (*R*)-**4** in the presence of Zn^{2+} is used to recognize chiral functional amines such as diamines, amino alcohols, and amino acids. It is found that the 2-naphthylamine unit of (*R*)-**4** can be released upon interaction with various chiral amine substrates in the presence of Zn^{2+} to exhibit fluorescence enhancement at two wavelengths in which one fluorescent signal is sensitive to the substrate concentration and the other is sensitive to the enantiomeric composition. Thus, one measurement of the fluorescent response at these two emitting wavelengths allows the determination of both concentration and enantiomeric composition. This strategy will be used to develop enantioselective fluorescent sensors for other chiral molecules.

EXPERIMENTAL SECTION

Materials and General Procedures. ^1H and ^{13}C NMR spectra were measured on a Bruker AM400 NMR spectrometer. Proton chemical shifts of NMR spectra were given in ppm relative to internals reference TMS (^1H, 0.00 ppm). HRMS spectral data were recorded on a Bruker Daltonics Bio TOF mass spectrometer. Fluorescence emission spectra were measured on FluoroMax-4 Spectrofluorophotometer (HORIBA Jobin Yvon) at 298 K. Unless otherwise noted, materials were obtained from commercial suppliers and were used without further purification. The enantiomers of *trans*-1,2-cyclohexanediamine and alaninol were redistilled before use. The enantiomers of phenylglycinol and phenylalaninol were recrystallization from toluene. The amino acids were obtained from commercial suppliers and were used without further purification. All of the solvents were either HPLC or spectroscopic grade in the optical spectroscopic studies.

Preparation and Characterization of (*R*)-4. (*R*)-**2** (98.1 mg, 0.29 mmol) and 2-naphthylamine (123.1 mg, 0.87 mmol) were stirred in refluxing CH_2Cl_2/CH_3OH 2:1 for 24 h. After evaporation of the solvent, the crude product was stirred in CH_3OH at rt for 12 h. A yellow solid was collected by filtration and washed with CH_3OH (4 mL). After dried under vacuum, (*R*)-**4** was obtained in 72% yield (121.8 mg). $[\alpha]_D = -337$ (c = 0.1, CH_2Cl_2). ^1H NMR ($CDCl_3$, 400 MHz) δ 13.14 (s, 2H), 9.03 (s, 2H), 8.23 (s, 2H), 8.28 (d, J = 8 Hz, 2H), 7.85 (d, J = 8 Hz, 2H), 7.80 (d, J = 8 Hz, 2H), 7.27 (d, J = 8 Hz, 2H), 7.99−7.97 (m, 2H), 7.55−7.34 (m, 12H). ^{13}C NMR ($CDCl_3$, 100 MHz) δ 163.7, 154.6, 146.2, 135.9, 135.2, 134.0, 129.2, 129.0, 128.3, 127.9, 127.8, 127.2, 126.7, 126.4, 125.9, 125.0, 123.8, 123.6, 121.7, 116.9, 114.0. HRMS (ES+) calcd for $C_{42}H_{29}N_2O_2$ ($M + H^+$) 593.2224 and $C_{42}H_{28}N_2O_2Na$ ($M + Na^+$) 615.2043, found 593.2272 and 615.2094.

Preparation and Characterization of (*S*)-4. (*S*)-**2** (20.6 mg, 0.06 mmol) and 2-naphthylamine (25.8 mg, 0.18 mmol) were stirred in refluxing CH_2Cl_2/CH_3OH 2:1 for 24 h. After evaporation of the solvent, the crude product was stirred in CH_3OH at rt for 12 h. A yellow solid was collected by filtration and washed with CH_3OH (2 mL). After dried under vacuum, (*S*)-**4** was obtained in 64.5% yield (23 mg). $[\alpha]_D = 308$ (c = 0.1, CH_2Cl_2). ^1H NMR ($CDCl_3$, 400 MHz) δ 13.15 (s, 2H), 9.03 (s, 2H), 8.24 (s, 2H), 8.28 (d, J = 8 Hz, 2H), 7.99 (d, J = 2.4 Hz, 2H), 7.97 (d, J = 2.4 Hz, 2H), 7.85 (d, J = 7.6 Hz, 2H), 7.80 (d, J = 8 Hz, 2H), 7.53−7.34 (m, 12H). ^{13}C NMR ($CDCl_3$, 100

DOI: 10.1021/jacs.5b01049
J. Am. Chem. Soc. 2015, 137, 4517−4524

MHz) δ 163.7, 154.6, 146.2, 135.9, 135.2, 134.0, 129.2, 129.0, 128.3, 127.9, 127.8, 127.2, 126.7, 126.4, 125.9, 125.0, 123.8, 123.6, 121.7, 116.9, 114.0. HRMS (ES+) calcd for $C_{42}H_{29}N_2O_2$ ($M + H^+$) 593.2224 and $C_{42}H_{28}N_2O_2Na$ ($M + Na^+$) 615.2043, found 593.2223 and 615.1963.

■ ASSOCIATED CONTENT

Supporting Information

Detailed experiments and additional spectroscopic data. This material is available free of charge via the Internet at http://pubs.acs.org/.

■ AUTHOR INFORMATION

Corresponding Authors

*yushanshan@scu.edu.cn
*xqyu@scu.edu.cn
*lp6n@virginia.edu

Notes

The authors declare no competing financial interest.

■ ACKNOWLEDGMENTS

This work was financially supported by the National Program on Key Basic Research Project of China (973 Program, 2012CB720603, 2013CB328900), and the National Science Foundation of China (nos. 21232005, 21321061 and J1103315).

■ REFERENCES

(1) For reviews on enantioselective fluorescent recognition: (a) Pu, L. *Chem. Rev.* **2004**, *104*, 1687−1716. (b) Leung, D.; Kang, S. O.; Anslyn, E. V. *Chem. Soc. Rev.* **2012**, *41*, 448−479. (c) Accetta, A.; Corradini, R.; Marchelli, R. *Top. Curr. Chem.* **2011**, *300*, 175−216. (d) Zhang, X.; Yin, J.; Yoon, J. *Chem. Rev.* **2014**, *114*, 4918−4959.

(2) Selected publications: (a) James, T. D.; Sandanayake, K. R. A. S.; Shinkai, S. *Nature* **1995**, *374*, 345−347. (b) Lin, J.; Hu, Q.-S.; Xu, M. H.; Pu, L. *J. Am. Chem. Soc.* **2002**, *124*, 2088−2089. (c) Zhao, J.-Z.; Fyles, T. M.; James, T. D. *Angew. Chem., Int. Ed.* **2004**, *43*, 3461−3464. (d) Zhu, L.; Anslyn, E. V. *J. Am. Chem. Soc.* **2004**, *126*, 3676−3677. (e) Mei, X. F.; Wolf, C. *J. Am. Chem. Soc.* **2004**, *126*, 14736−14737. (f) Pu, L. *Acc. Chem. Res.* **2012**, *45*, 150−163.

(3) (a) Mei, X. F.; Wolf, C. *J. Am. Chem. Soc.* **2006**, *128*, 13326−13327. (b) Bentley, K. W.; Wolf, C. *J. Am. Chem. Soc.* **2013**, *135*, 12200−12203. (c) Zhu, L.; Anslyn, E. V. *J. Am. Chem. Soc.* **2004**, *126*, 3676−3677. (d) Shabbir, S. H.; Joyce, L. A.; da Cruz, G. M.; Lynch, V. M.; Sorey, S.; Anslyn, E. V. *J. Am. Chem. Soc.* **2009**, *131*, 13125−13131. (e) Wolf, C.; Liu, S.; Reinhardt, B. C. *Chem. Commun.* **2006**, *48*, 4242−4244. (f) Nieto, S.; Lynch, V. M.; Anslyn, E. V.; Kim, H.; Chin, J. *J. Am. Chem. Soc.* **2008**, *130*, 9232−9233. (g) Nieto, S.; Lynch, V. M.; Anslyn, E. V.; Kim, H.; Chin, J. *Org. Lett.* **2008**, *10*, 5167−5170. (h) Nieto, S.; Dragna, J. M.; Anslyn, E. V. *Chem.—Eur. J.* **2010**, *16*, 227−232.

(4) (a) Yu, S. S.; Pu, L. *J. Am. Chem. Soc.* **2010**, *132*, 17698−17700. (b) Yu, S. S.; Plunkett, W.; Kim, M.; Pu, L. *J. Am. Chem. Soc.* **2012**, *134*, 20282−20285. (c) Huang, Z.; Yu, S. S.; Zhao, X.; Wen, K. L.; Xu, Y. M.; Yu, X. Q.; Xu, Y.; Pu, L. *Chem.—Eur. J.* **2014**, *20*, 16458−16461.

(5) Huang, Z.; Yu, S. S.; Wen, K. L.; Yu, X. Q.; Pu, L. *Chem. Sci.* **2014**, *5*, 3457−3462.

DOI: 10.1021/jacs.5b01049
J. Am. Chem. Soc. 2015, 137, 4517−4524